

ILC-Asia-2007-02  
Sep. 17, 2007  
Linac, Cavity, Detuning

# **Estimation of Transient Lorentz Detuning of ICHIRO Cavity with Helium Jacket**

T. Higo (KEK), et al.

# Estimation of Transient Lorentz Detuning of ICHIRO Cavity with Helium Jacket

T. Higo<sup>1</sup>, F. Furuta<sup>1</sup>, Y. Higashi<sup>1</sup>, Y. Morita<sup>2</sup>, Y. Morozumi<sup>1</sup>, T. Saeki<sup>1</sup>, H. Yamaoka<sup>1</sup> and  
K. Saito<sup>1</sup>

<sup>1</sup> KEK, High Energy Accelerator Research Organization  
1-1, Oho, Tsukuba, Ibaragi, 305-0801, Japan

<sup>2</sup> International Center for Elementary Particle Physics, ICEPP, The University of Tokyo  
7-3-1 Hongo, Bunkyo-ku, Tokyo, 113-0033, Japan

## Abstract

In our previous paper, the Lorentz detuning was calculated for a low-loss cavity, the ICHIRO cavity, being developed for ILC, in a condition that both ends of the cavity were fixed in the axial direction. In the present paper, the transient detuning was further estimated in a more practical configuration, where both ends of the cavity were connected by a Helium vessel and the end plates.

The total amount of the detuning increases by only 8 % with respect to that with both ends fixed. The total amount at the flat top becomes 2.6 kHz at 45MV/m, corresponding to the sensitivity of  $1.28 \text{ Hz}/(\text{MV}/\text{m})^2$ . The time profile of the detuning follows that of  $E_{\text{acc}}^2$ . A higher frequency (1.3 kHz) modulation of only a few percent level was identified. This oscillation was found due to the axial motion of each cell.

The total amount of the detuning was found roughly consistent to the sum of the two components, one due to the single cell deformation of  $\sim 1700\text{Hz}$  and the other from the multi-cell deformation  $\sim 750\text{Hz}$ .

## 1. Introduction

The suppression and compensation of the big Lorentz detuning is still one of the main issues for realizing the ILC<sup>1</sup>.

One of the ways to estimate the transient behavior of the detuning is to analyze the mechanical resonances of the system, calculating the resonant modes and the coupling to the electromagnetic pressure (Maxwell's stress) due the stored field in the cavity<sup>2,3</sup>. In the reference 3, the Lorentz detuning was well estimated with up to the 4<sup>th</sup> mode in a single cell, while in the reference 2 five-cell cavity was analyzed and found that only the modes below 8 kHz have large coupling to the excited electromagnetic field. The compensation by the fast Piezo device can also estimated by the same method based on the mechanical resonance modes and their coupling to the fast tuner movement<sup>4</sup>.

On the other hand in our previous paper<sup>5</sup>, the Lorentz detuning and the transient tuning behavior for ICHIRO cavity<sup>6</sup> was estimated based on a direct time-domain analysis of the cavity system. In this analysis, the time-dependent deformation of the 9-cell cavity was performed with the code ANSYS<sup>8</sup> and the frequency detuning was calculated from the sum of the frequency detuning of each cell using Slater's perturbation technique. The most practical estimation in the paper was that for the case with both end flanges of the 9-cell cavity fixed in the axial direction. However, in the actual configuration, both ends are mechanically connected with a finite stiffness, though as much as a factor 10 larger stiffness than that of cavity itself. This results in a little bigger detuning amount. In the present paper, we calculated again the Lorentz detuning in the same manner as before but in such a practical mechanical constraint.

## 2. Mechanical configuration of ICHIRO cavity

### *ICHIRO cavity shape*

The ICHIRO cavity shape is shown in Fig. 1<sup>6</sup>. The left side is called “inner side” and the right side “outer side” in this note. We name the cells from the left end cell to the right end cell as from #1 to #9. Cell dimensions are summarized in <http://lcdev.kek.jp>.

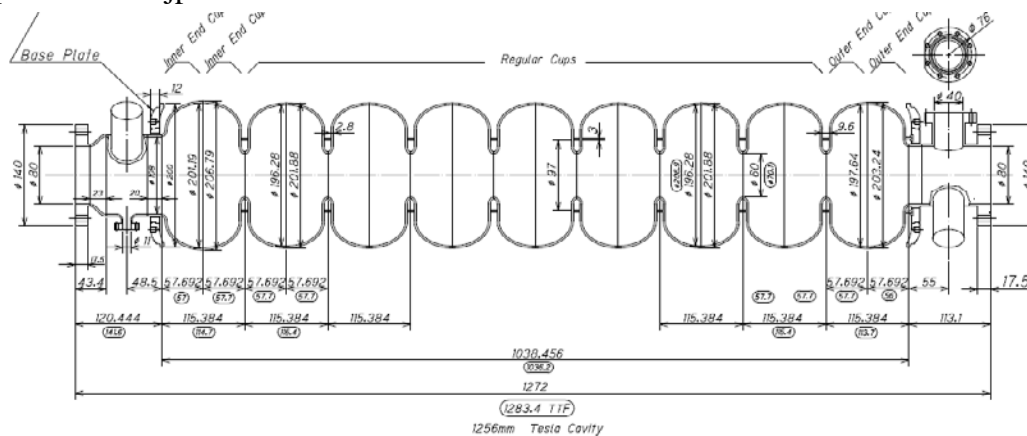


**Fig. 1 Bare ICHIRO cavity.**

### *Practical configuration with a cavity with Helium vessel*

The actual cavity geometry with the Helium vessel is shown in Fig. 2. The Helium jacket is made of stainless steel with its thickness of 3mm. This connects beam pipes of both cavity ends through the stainless steel end plates with the thickness of 10mm.

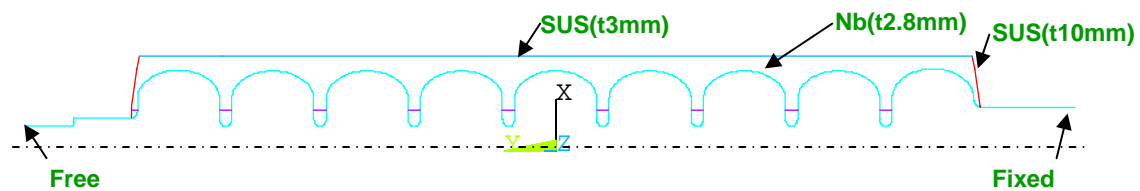


**Fig. 2 Configuration for calculation of cavity with Helium jacket.**

### 3. Applied RF pulse shape and mechanical movement

The accelerating field of the cavity is assumed to vary graphically shown in Fig. 3. The actual functional form<sup>7</sup> is as shown below.

$$E_{acc}(t)^2 = E_{acc}^0{}^2 * (1 - \text{Exp}(-\omega t / 2Q_L))$$

where  $1/Q_L = 1/Q_0 + 1/Q_{ex}$

We set values,  $E_{acc}^0 = 45\text{MV/m}$ ,  $Q_0 \gg Q_{ex} = 2.6 \times 10^6$ . The ramping period is 0.571msec.

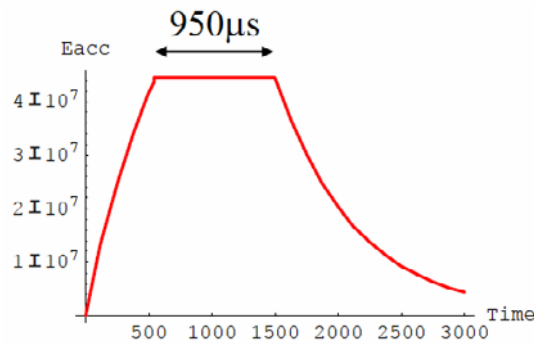


Fig. 3 Acceleration field versus time.

The mechanical movement of the system was calculated by ANSYS<sup>8</sup> in time domain. The points for monitoring mechanical movement are shown in Fig. 4. The result is shown in Fig. 5.

It was observed that during the pulse most of the points were shrunk in the axial direction in a proportional manner to the distance from the fixed point at the right end. This is the breathing mode and we speculate that this overall shrinkage results in the frequency decrease. In addition to this movement, we note that the frequency component of about 1.3 kHz (evaluated by eye) develops from fairly early stage of the pulse and it stays even after pulse ends with the amplitude maximum at the center region in 9-cell cavity. From the nature of this movement pattern, we speculate that this oscillation does not affect frequency much since the total length of the cavity stays constant.

In contrast to the axial movement, the radial movements for all of the cells show a very simple pattern, which is close to the Maxwell's stress. The flat-top amount is 0.2μm at 45MV/m. This value results in the frequency detuning of roughly 2.6 kHz assuming the sensitivity in a pillbox with its radius of 100mm resonating at 1.3 GHz.

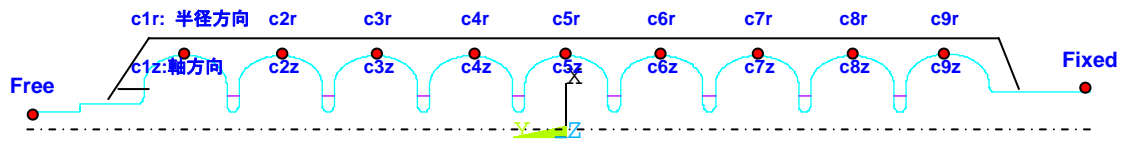


Fig. 4 Monitor points for mechanical movements.

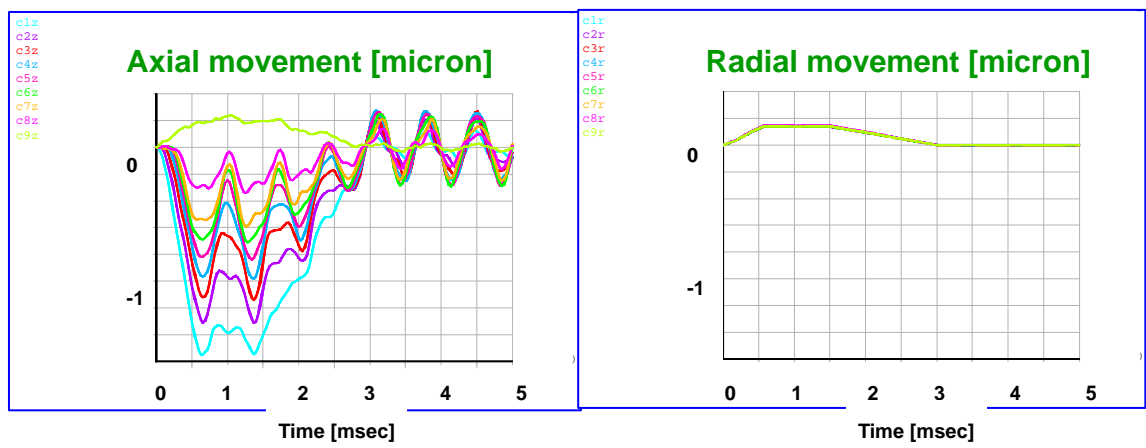


Fig. 5 Mechanical movement of monitor points versus time at 38.4MV/m.

## 4. Calculation of Lorentz detuning

The amount of the Lorentz detuning for each cell was calculated summing the frequency perturbation within each cell. The result is shown in Fig. 6. It is noted that the effect is large at the end cell and the adjacent cells, especially during the RF pulse exists. The frequency detunings of all of the cells are summed to obtain the total frequency detuning of a cavity<sup>9</sup>. The result is shown in Fig 7.

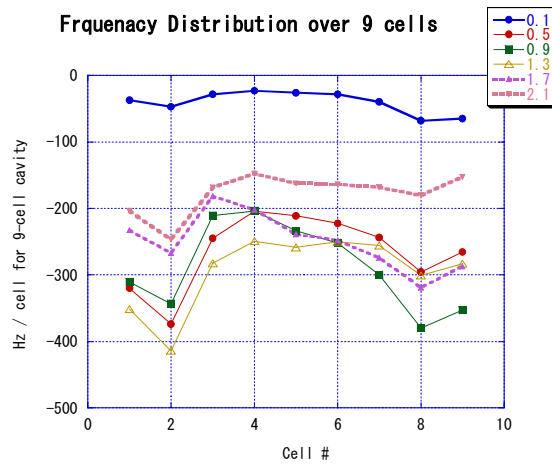


Fig. 6 Each cell frequency detuning at various timing of the pulse.

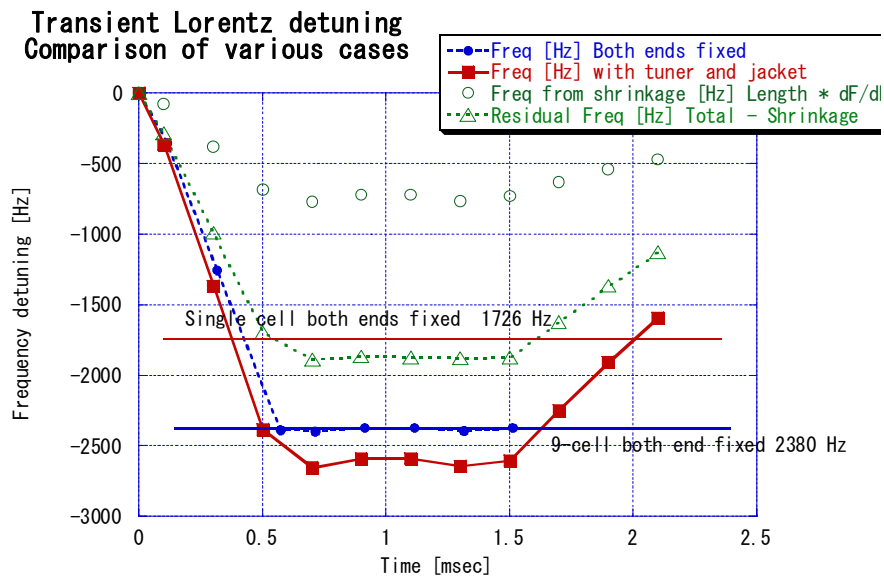


Fig. 7 Total frequency detuning along the pulse for the flat top of 45MV/m.

It is to be noted that the shape almost follows that of  $E_{acc}^2$  and its amplitude is also close to that estimated from the deformation in the radial direction as described in the previous section. Small wiggling of a few percents level is seen in the flat top region. The frequency of this ripple is about 1.3 kHz, which attributes to the axial deformation shown in Fig. 5. The decaying part does not follow  $E_{acc}^2$  but decays in a slowly manner, which is not clearly understood. In summary, the relevant values on the Lorentz detuning are listed in the Table 1.

Table 1 Results of Lorentz detuning calculation.

Flat-top value	At 45MV/m	At 31.5MV/m	Sensitivity
	Hz	Hz	Hz / (MV/m) <sup>2</sup>
Single-cell <sup>(a)</sup>	1726	846	0.85
Total amount in 9-cell			
Both ends fixed in Z <sup>(b)</sup>	2380	1170	1.18
End plates fixed by He vessel	2600	1274	1.28
Total length $\delta l$	1.7 $\mu$ m		
$\rightarrow$ Freq. $df/dl * \delta l$	$\rightarrow$ 630 Hz		
Cell radius	0.2 $\mu$ m		
$\rightarrow$ Freq. $df/dr * \delta r$	$\rightarrow$ 2600 <sup>(c)</sup>		

(a) Detuning of a single cell with both iris fixed in z-direction<sup>5</sup>.

(b) from ref<sup>5</sup>.

(c) Assuming the sensitivity of  $df/dr = 1.3\text{GHz} / 100\text{mm}$ . Actually the sensitivity should be smaller due to the actual shape different from pillbox.

## 5. Summary and discussions

The detuning amount versus time is decomposed as below. The total amount at the flat top area is 2.6kHz at 45MV/m operation, corresponding to the sensitivity of  $1.28 \text{ Hz}/(\text{MV}/\text{m})^2$ .

The total shrinkage is measured as the distance between two flanges. The frequency shift due to this shrinkage is calculated by multiplying 368Hz/micron. The result is shown in green open circle. It follows roughly  $E_{\text{acc}}^2$ . This shrinkage effect shows an oscillatory characteristic at the flat top. This variation results in a modulation of the total detuning amount at the flat top area. The frequency of this variation is consistent with that of mechanical oscillation at about 1.3 kHz shown in Fig. 5.

The residual amount, total – shrinkage, is shown in green open triangle. The amount of this residual at the flat top is close to the single cell frequency detuning with both ends fixed, which was calculated to be 1726Hz in reference<sup>5</sup>.

From the above decomposition, it is noted that the total detuning amount consists of two parts, one due to the single cell detuning with each cell length kept constant and the second multi-cell detuning with varying the cell length.

The total frequency detuning with both ends fixed is shown in the same figure with blue solid circles which was calculated in our previous paper<sup>5</sup>. The increase of detuning amount from that with fixed ends to that of the present configuration of both ends connected through Helium jacket should be attributed to the finite stiffness of the Helium jacket and end plates. The total shrinkage amount of  $1.7\mu\text{m}$  at 45MV/m is consistent with that estimated from the stiffness of the cavity system with vessel and the axial force 103N due to Maxwell stress. However, this shrinkage corresponds to 635Hz which is much larger than the difference of our estimations from the flat-top value with both ends fixed to that with a practical configuration with Helium jacket. This disagreement is not understood and should be carefully re-examined to understand the mechanism of the detuning.

The basic deformation characteristics should be understood based on the mechanical mode analysis. Some analyses are already ongoing as shown in the references<sup>10,11</sup> and we hope to understand the result of the present data with a clear physical view.

## References

- 
- <sup>1</sup> ILC Web site, <http://www.linearcollider.org/cms/>.
  - <sup>2</sup> G. Devanz et al., “Numerical Simulations of Dynamic Lorentz Detuning of SC Cavities,” p2220, Proc. EPAC 2002, Paris, France, 2002.
  - <sup>3</sup> E. Chishiro et al., “Modelling of Resonant Frequency Vibration of Superconducting Cavity”, p41, Proc. 2<sup>nd</sup> Superconducting Linear Accelerator Meeting in Japan,” KEK, Tsukuba, Japan, 1999, in Japanese.
  - <sup>4</sup> M. Luong et al., “Minimizing RF Power Requirement and Improving Amplitude/Phase Control for High Gradient Superconducting Cavities”, p2265, Proc. EPAC 2002, Paris, France, 2002.
  - <sup>5</sup> T. Higo et al., ILC-Asia Note 2006-01, “Estimation of Lorentz detuning and related tuning characteristics on ICHIRO cavity,” <http://lcdev.kek.jp/>
  - <sup>6</sup> Detailed information of ICHIRO cavity can be retrieved in Morozumi’s talk in 7<sup>th</sup> WG5-Asia meeting on 17 Dec. 2004, <http://lcdev.kek.jp/ILC-AsiaWG/WG5notes/>.
  - <sup>7</sup> Y. Morozumi, 17<sup>th</sup> WG5 meeting, <http://lcdev.kek.jp/ILC-AsiaWG/WG5notes/>, June, 2005.
  - <sup>8</sup> ANSYS, <http://www.ansys.com/>
  - <sup>9</sup> T. Higo and H. Yamaoka, “Transient Lorentz Detuning (2)”, <http://lcdev.kek.jp/ILC-AsiaWG/WG5notes/>, Oct. 20, 2006
  - <sup>10</sup> Y. Morozumi, private communication.
  - <sup>11</sup> M. Yamamoto, <http://www.akita-nct.jp/yamamoto/study/collaboration/KEK/>